A New Hypo-Rayleigh Distribution for Short Range Wide-Band Directive Indoor Channel Fading Modeling at 3.3 and 5.5 GHz Bands

Bazil Taha Ahmed, bazil.taha@uam.es, Miriam Esteban Plaza

Escuela Politécnica Superior

Universidad Autónoma de Madrid- SPAIN

Abstract: In this work, propagation loss models for indoor environment are presented. The directive channel propagation loss in indoor environment at frequency bands of 3.3 GHz with a channel bandwidth of 200 MHz and 5.5 GHz band with 320 MHz bandwidth is measured using vertical polarizations where a set of directive panel antennas and a network analyzer are used in the measurement campaign. It is noticed that, the propagation loss can be modelled by two slopes propagation model giving a rise to two propagation zones. The first zone of propagation is almost free space propagation zone while generally; the second zone has a higher deviation from the mean value of propagation loss. A new Hypo-Rayleigh distribution is proposed to model the channel induced fading in the second zone of the propagation zones.

Keywords: Directive channel, propagation loss, Gaussian distribution, Rayleigh distribution, Hypo-Rayleigh distribution.

1 Introduction

The study of indoor propagation is of vital importance since it can be used in many applications, namely, indoor communications and localization [1-3]. In [4], a theoretical treatment of propagation in indoor environment has been given meanwhile in [5], a mode based approach for characterizing RF propagation in conduits has been given. Cut-off frequency of each mode of propagation has been obtained. In [6] indoor propagation loss at 2.4 GHz band has been presented. Studied zones are a closed corridor, an open corridor and a classroom. Results show that propagation loss deviation from the mean value can be presented by Gaussian distribution with $\sigma \approx 1$

dB for all the cases. In [7] propagation losses have been measured in different frequency bands (1, 2.4 and 5.8 GHz) within an arched cross section tunnels. Results have shown that fast fading could be represented by Rayleigh distribution. The used antennas were wideband horn antennas with a gain of 9.2 dBi at 2.4 GHz and 10.1 dBi at 5.8 GHz. In [8] propagation loss in narrow tunnels is presented. Measurements results at 374 MHz, 915 MHz, and 2400 MHz are given. Studied scenarios were unobstructed, line of site (LOS), Obstructed LOS, T-junction NLOS and L-bend NLOS. Results show that deviation from the mean value could be presented by Gaussian distribution. Antennas used at 2.4 GHz, have a gain of 6.5 dBi. In [9], different propagation models for coverage prediction of WiMAX microcellular and picocellular urban environments and for WiMAX indoor femtocells at 3.5 GHz are compared with experimental data. Results obtained for different urban and indoor environments show that statistical models are quite far from good agreement with experimental data while deterministic ray-tracing models provide appropriate prediction in all different complex analyzed environments. The modeling of new WLAN models for indoor and outdoor environments is presented in [10]. Based on the standard OPNET models for WLAN nodes, the propagation loss estimation for these two types of environment has been improved. Paper [11] describes and evaluates a new algorithm for the purpose of Indoor propagation prediction for centimetric waves. The approach shown in this paper started from formalism similar to the famous transmission line model approach in the frequency domain. In [12], the radio channel characterization of an underground mine at 2.4 GHz has been investigated. Propagation loss as a function of the distance between the transmitter and the receiver has been presented. Delay spread has been also given. In [13], the propagation modes and the temporal variations along a lift shaft in UHF band have been given. Moreover, propagation in corridors, as well as tunnels and urban street canyons has been studied in [14, 15]. In [14], the radio wave propagation from an indoor hall to a corridor was studied by analyzing the results from a multi-link MIMO channel sounding measurement. The results showed that despite NLOS conditions, the dominant propagation mechanisms comprised direct path through the wall and specular reflections. In [15], the different propagation mechanisms associated with the lift shaft have been studied in detail. Analysis of the measurement results verified the presence of electromagnetic waves being guided along the lift shaft. The guiding effect of the lift shaft has been an important propagation

mechanism. In [16], the propagation loss for indoor scenarios has been given at 5.5 GHz band where antennas with different gains have been used in the propagation loss measurements. In [17], the narrowband short range directive channel propagation loss in indoor environment at 2.4 GHz, 3.3 GHz and 5.5 GHz bands has been studied. It has been noticed that the propagation loss can be modelled by a single slope propagation model or two slopes propagation model.

The main contribution of this paper is to propose a new Hypo-Rayleigh distribution to model to the indoor directive channel at 3.3 GHz and 5.5 GHz bands.

The rest of the paper is organized as follows. In Section 2, the propagation models for indoor environment are given. In Section 3, the measurement setup is described. Results are given in Section 4. Finally Section 5 addresses the conclusions.

2   Propagation model

In open zones, the two ray propagation model (the direct ray and the surface reflected ray) is used to calculate the propagation loss. The 2-Ray ground reflected model may be thought as a special case of multi-slope model with break point at critical distance with slope 20 dB/ decade before the critical distance and slope of 40 dB/ decade after the critical distance.

In indoor environment, propagation could be due to the direct ray and four reflection rays (reflection from side walls, ground and ceil). For a medium distance (higher than the width of the studied zone) between the transmitting antenna and the receiving one, multi reflection rays may are also exists. Thus, in general, indoor propagation cannot be represented by the Two Rays Model (direct ray and ground reflection one).

For a short distance between the transmitting and receiving antennas (d), the propagation loss for an indoor environment is represented by the single slope propagation model given by:

$$L_p = L_o + 10\, n_1 \log_{10}\left(\frac{d}{d_o}\right) + \xi_1 \qquad\qquad (1)$$

, where L_o is the propagation loss at the reference distance do (1 m in our case), n_1 is the propagation exponent, and ξ_1 is a random variable (Gaussian (G), Rayleigh (R) or a combination of both) that represents the deviation from the mean value [16]. For

directive channels ξ_1 can be represented by (Gaussian (G), or Hypo-Rayleigh (HR) distribution [See appendix A] or a combination of both.

For a higher distance between the transmitting antenna and the receiving one, a second propagation exponent n_2 is observed, thus the propagation loss will be presented by the two slope model. The change from n_1 to n_2 occurs at the break point at a distance R_b. Thus, the propagation loss can be written as:

$$L_p(dB) = \begin{cases} L_o + 10\, n_1 \log_{10}(d_b) + \xi_1, & d \leq R_b \\ L_1 + 10\, n_2 \log_{10}\left(\dfrac{d}{R_b}\right) + \xi_2, & d > R_b \end{cases} \tag{2}$$

, where L_1 is the propagation loss of the distance R_b at which the propagation exponent changes to n_2, n_2 is the second propagation n_2 and ξ_2 is a random variable (Gaussian, Rayleigh or a combination of both) that represents the deviation from the main value [16]. For directive channels ξ_2 can be represented by Hypo-Rayleigh (HR) distribution. The propagation exponent n_2 could have a value higher or lower than 2 depending on the studied scenario.

The random variables ξ_1 and ξ_2 can be presented by:

$$\xi_{1,2} = \sum_{n=1}^{N} W_{G,n} \quad G_n(\mu, \sigma) + W_R \ R \tag{3}$$

Where

- $W_{G,n}$ is the weight of the Gaussian component n
- W_R is the weight of the Rayleigh component R

For directive channels, the random variables ξ_1 and ξ_2 can be presented by:

$$\xi_{1,2} = \sum_{n=1}^{N} W_{G,n} \quad G_n(\mu, \sigma) + W_{HR} \ HR \tag{4}$$

Where

- $W_{G,n}$ is the weight of the Gaussian component n
- W_{HR} is the weight of the Hypo-Rayleigh component

Or it can be presented by only Hypo-Rayleigh (HR) distribution.

3 Measurement equipments

For the studied scenario, a portable Network Analyzer (6 GHz ZVL of Rohde & Schwarz) has been used to measure the propagation loss up to 20 m. The output power in all the measurements was 20 dBm, with a receiver resolution bandwidth of 100 KHz, and the Rx antenna is separated from the Tx antenna (fix) from 1 to 20 m. Measurements are carried out with different antenna heights of both transmitting and receiving antennas moving the receiving antenna progressively farther from the transmitting one in steps of 0.25 m. Channel band has been selected to be 200 MHz at the 3.3 GHz band and 320 MHz at the 5.5 GHz band. The used antennas have a gain of 15 dB each one. The number of measurement points within the bandwidth is 1001 frequency points.

Measurements have been carried out within the Escuela Politecnica Superior of the Universidad Autónoma de Madrid. Fig. 1 illustrates the measurement system set up.
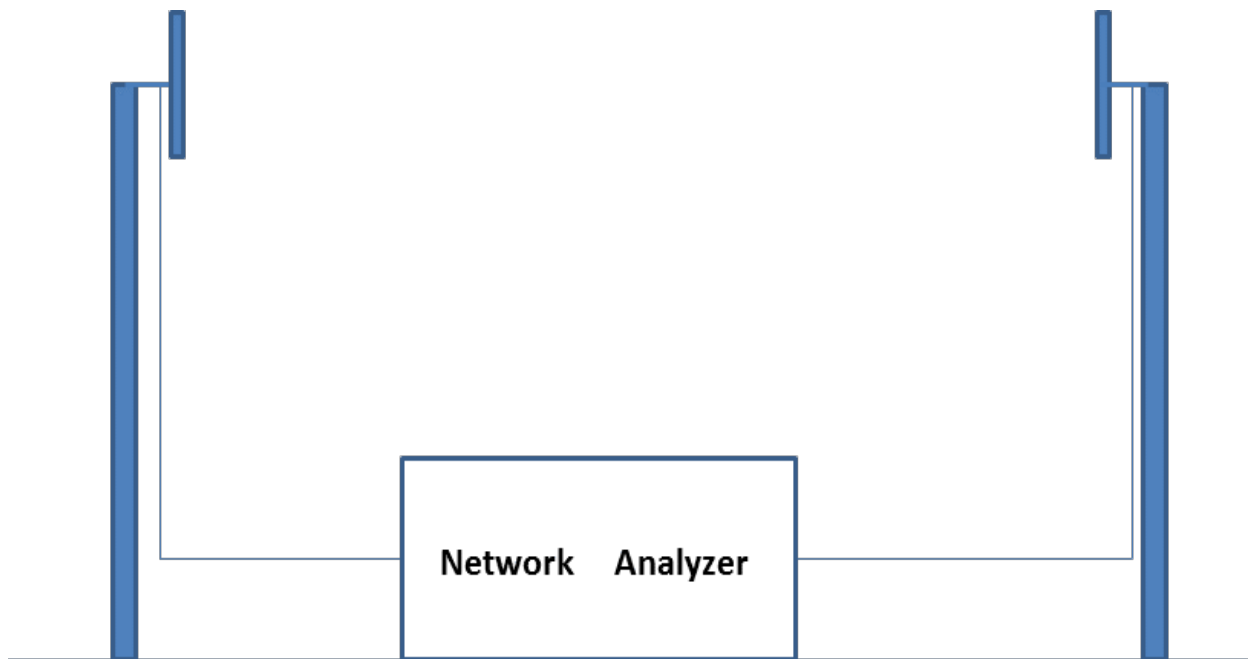
Fig. 1: Measurement setup.

4 Measurement results

The studied scenario is represented by Fig. 2(a) and a photograph of it is given by Fig. 2(b). It consists of 7.2 m passage with a length of 60 m. Measurements have been carried out with a maximum distance between the two antennas (transmitting and receiving one) of 20 m.
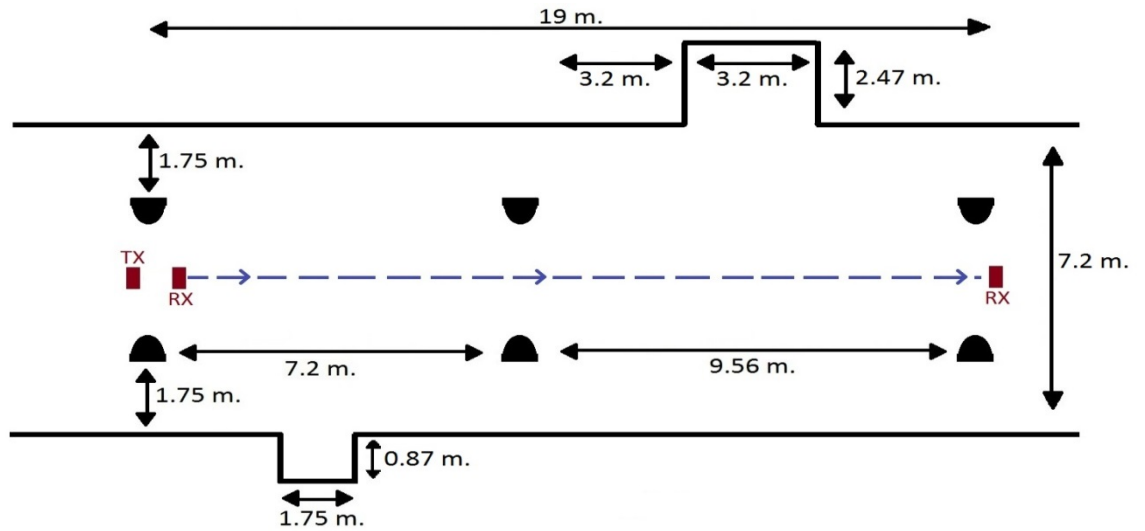
(a)

(a) Layout of the studied scenario.

(b)

(b) Photograph of the studied scenario.

Fig. 2: Studied scenario.

The Rayleigh induced fading can be encountered when omnidirectional antennas are used for both transmitting and receiving in a rich scattering environment without any direct ray between transmitting and receiving antennas. When directional antennas are used for transmission and reception giving a rise to strong line of sight direct ray, the Rayleigh induced fading reduces to Hypo-Rayleigh induced fading.

Firstly we will present the result for an antenna height of 1 m and a frequency band of 3.3 GHz. Figure (3) shows the propagation gain of the directive channel. Two zones can be distinguished. The first one is with a propagation exponent n_1 of 1.866 and the second one with a propagation exponent n_2 of 1.775. **The propagation exponents have been found using the Least Square Fitting.** In the first zone, the induced fading can be approximated by a Gaussian distribution with $\mu = 0$ and $\sigma = 0.8$ dB. The induced fading of the second zone is approximated by a Gaussian distribution with ($\mu = 0$ dB, σ

7

= 2.5 dB) as shown in Figure 4. Also, the induced fading of the second zone is approximated by a Hypo-Rayleigh distribution (with a = 0.316 and σ = 0.5) as shown in Figure 5. **The existence of the Hypo-Rayleigh induced fading is due the fact that there is a strong direct ray between the transmitting antenna and the receiving one. This makes the induced Rayleigh fading inapplicable in our case.**
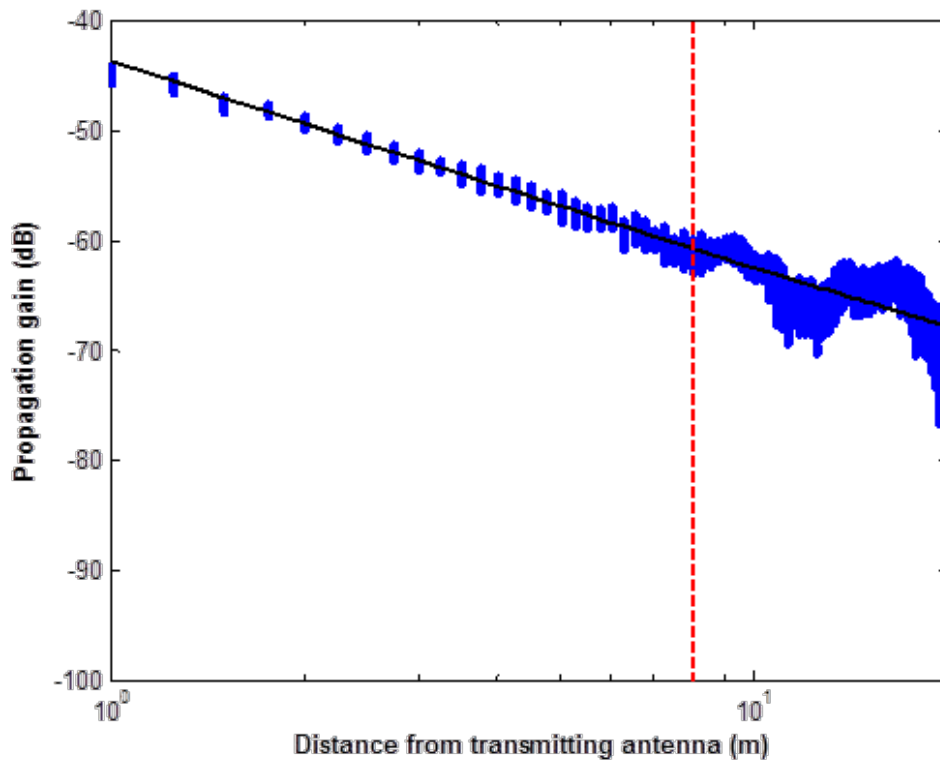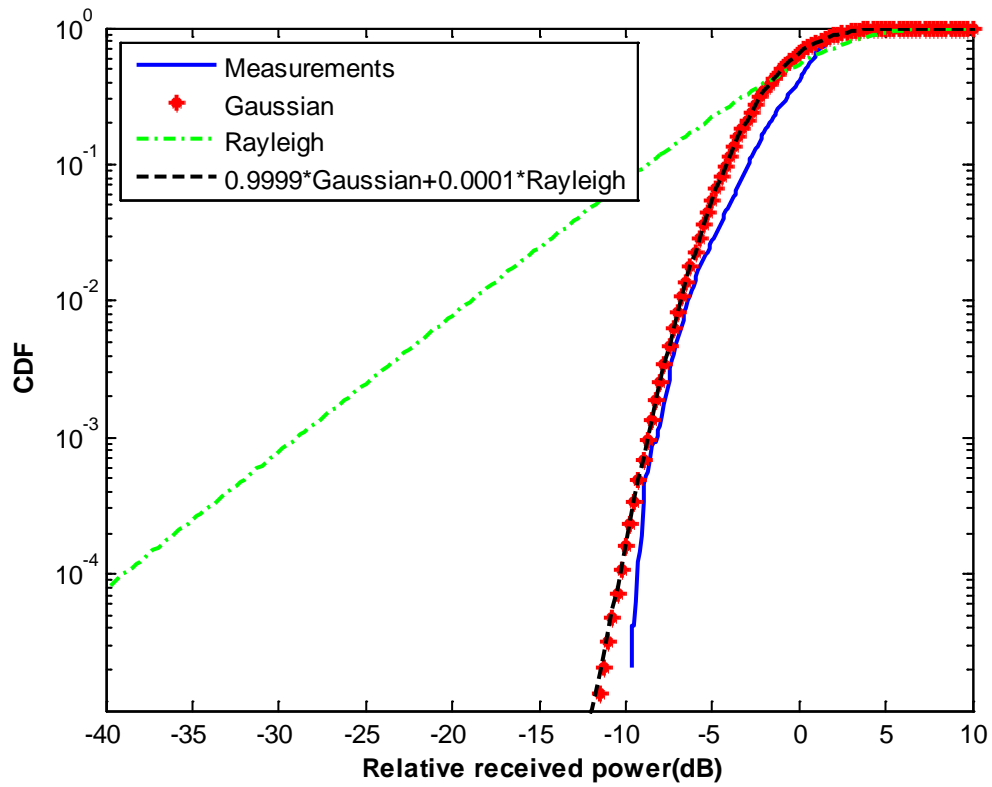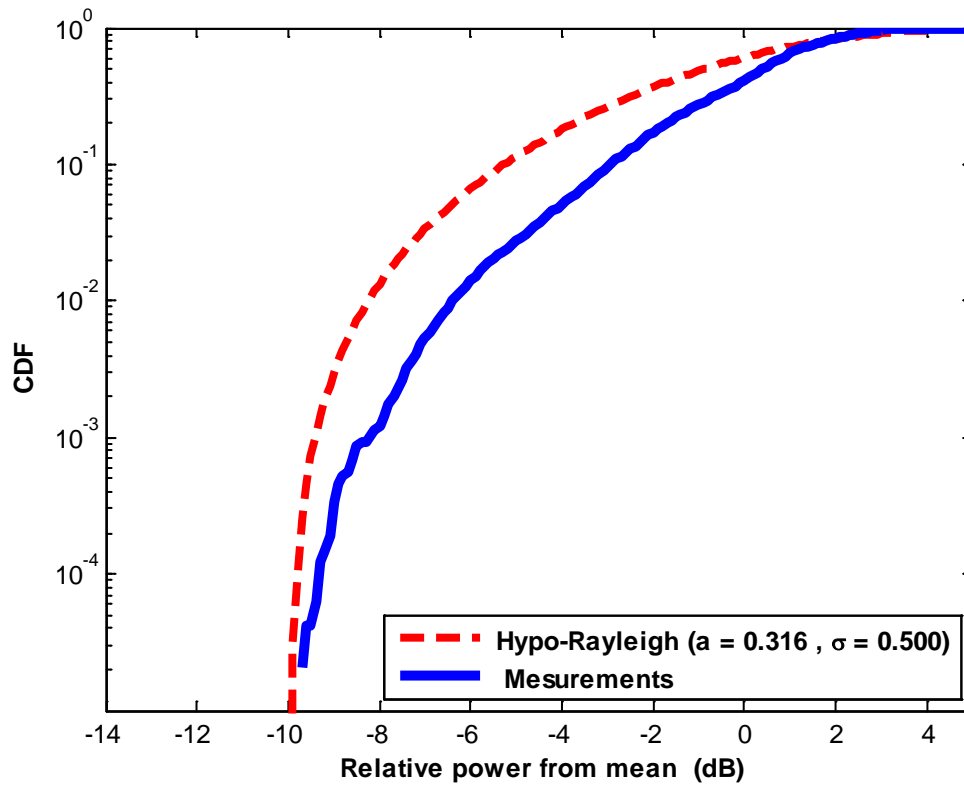

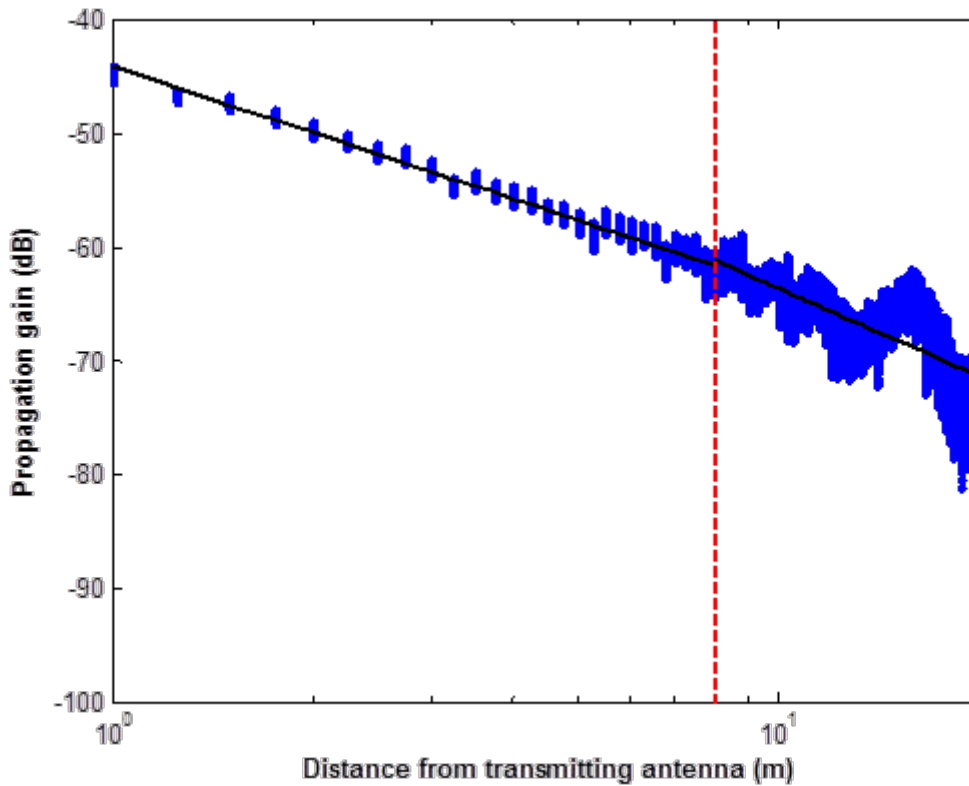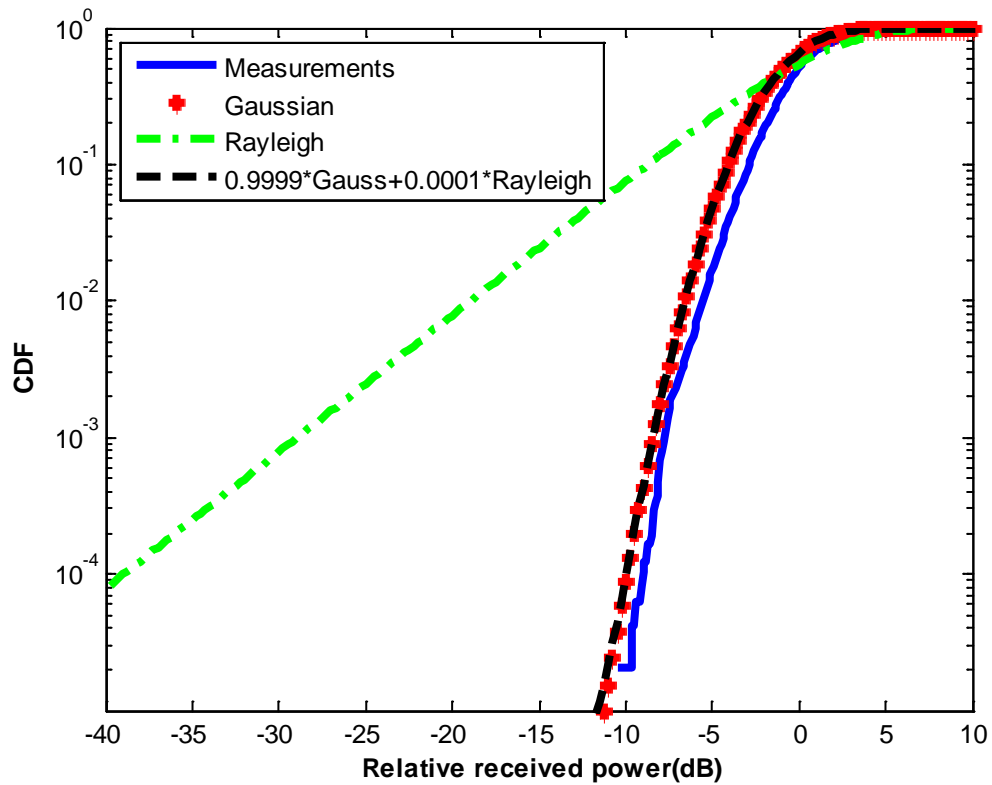**Fig. 3:** Propagation gain at antenna height of 1 m.

Fig. 4: CDF of the induced fading of the second zone approximated by Gaussian distribution with ($\mu = 0$ dB, $\sigma = 2.5$ dB) for antenna height of 1 m.

Fig. 5: CDF of the induced fading of the second zone approximated by a Hypo-Rayleigh distribution for antenna height of 1 m.

Secondly we will present the result for an antenna height of 1.4 m and a frequency band of 3.3 GHz.

Figure (6) shows the propagation gain of the directive channel. Two zones can be distinguished. The first one is with a propagation exponent n_1 of 1.932 and the second one with a propagation exponent n_2 of 2.562. The propagation exponents have been found using the Least Square Fitting. In the first zone, the induced fading can be approximated by a Gaussian distribution with $\mu = 0$ and $\sigma = 0.8$ dB. The induced fading of the second zone is approximated by a Gaussian distribution with ($\mu = 0$ dB, $\sigma = 2.4$ dB) as shown in Figure 7.

Also, the induced fading of the second zone is approximated by a Hypo-Rayleigh distribution (with a = 0.3 and $\sigma = 0.5$) as shown in Figure (8). Here also the existence of the Hypo-Rayleigh induced fading is due the fact that there is a strong direct ray between the transmitting antenna and the receiving one. This also makes the induced Rayleigh fading inapplicable in our case.

Fig. 6: Propagation gain at antenna height of 1.4 m.

Fig. 7: CDF of the induced fading of the second zone approximated by Gaussian distribution with (μ = 0 dB, σ = 2.4 dB) for antenna height of 1.4 m.
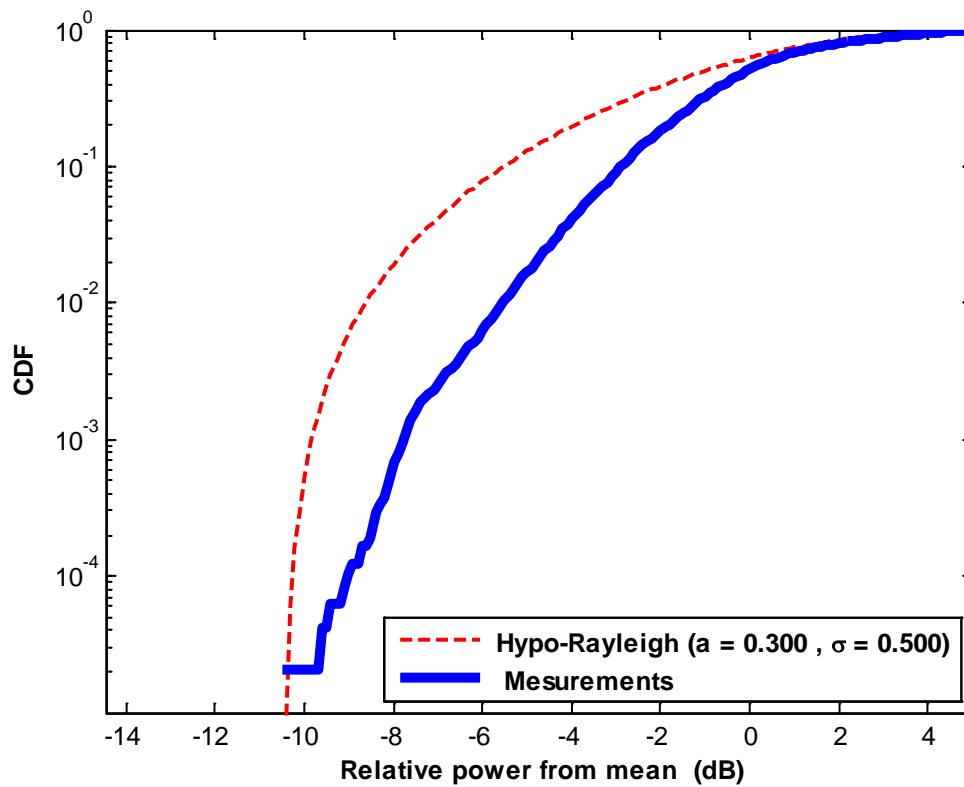
Fig. 8: CDF of the induced fading of the second zone for antenna height of 1.4 m.

Thirdly we will present the result for an antenna height of 1.8 m and a frequency band of 3.3 GHz.

Figure (9) shows the propagation gain of the directive channel. Two zones can be distinguished. The first one is with a propagation exponent n_1 of 1.851 and the second one with a propagation exponent n_2 of 1.898. The propagation exponents have been found using the Least Square Fitting. In the first zone, the induced fading can be approximated by a Gaussian distribution with $\mu = 0$ and $\sigma = 1$ dB. The induced fading of the second zone is approximated by a Gaussian distribution with ($\mu = 0$ dB, $\sigma = 2.1$ dB) as shown in Figure 10. Also, the induced fading of the second zone is approximated by a Hypo-Rayleigh distribution (with $a = 0.4$ and $\sigma = 0.45$) as shown in Figure (11).

In all of the cases, the break point distance is 8 m.

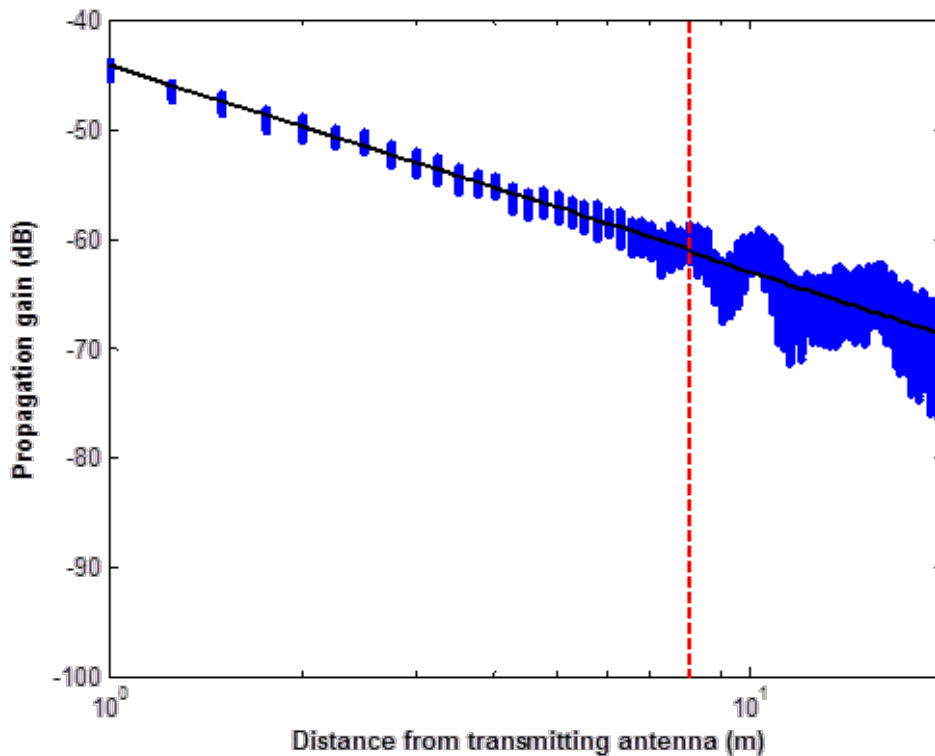It can be noticed that increasing the antenna height reduces the fading severity.

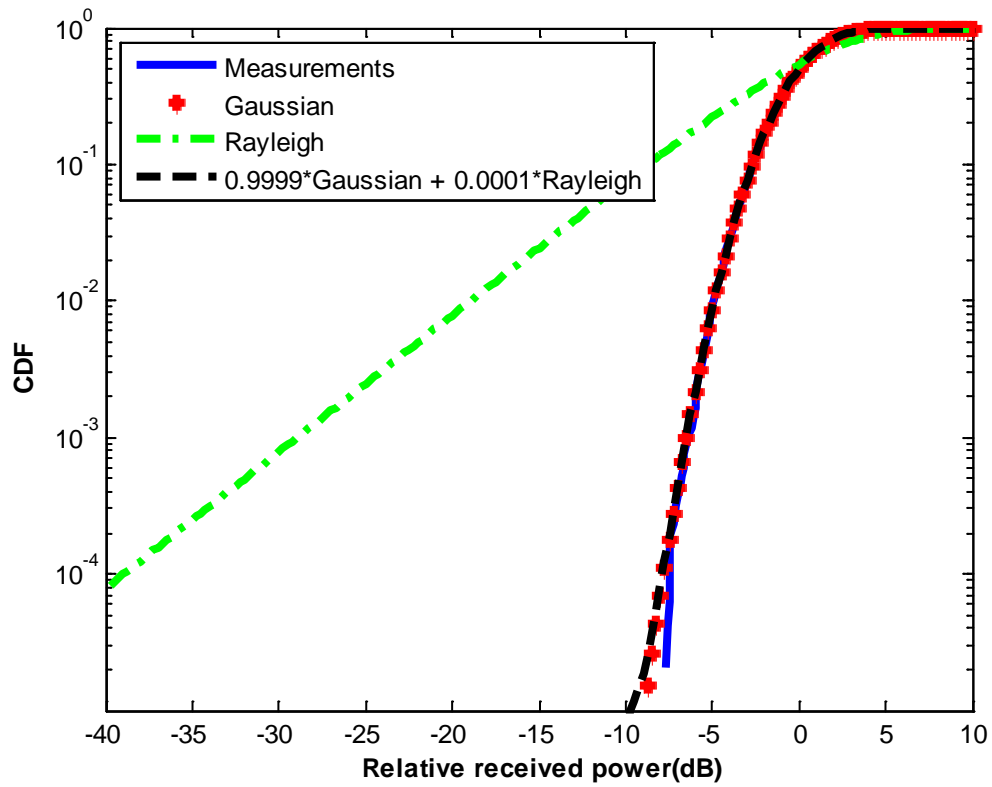
Fig. 9: Propagation gain at antenna height of 1.8 m.

Fig. 10: CDF of the induced fading of the second zone approximated by Gaussian distribution with (μ = 0 dB, σ = 2.1 dB) for antenna height of 1.8 m.
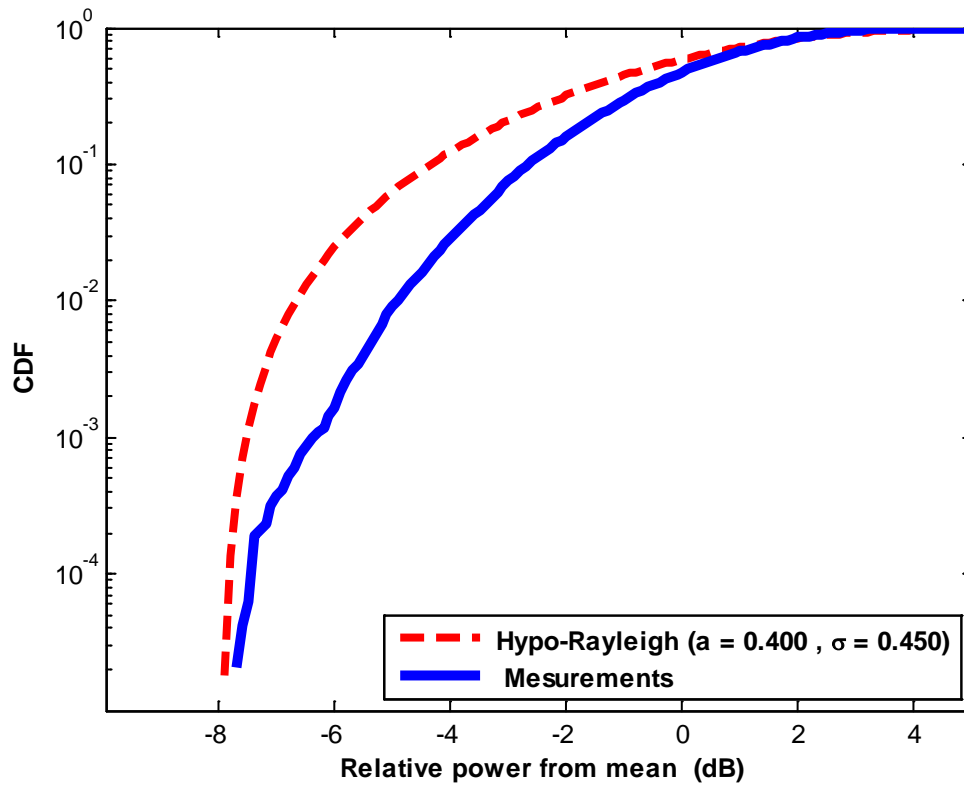
Fig. 11: CDF of the induced fading of the second zone for antenna height of 1.8 m.

Fourthly we will present the result for an antenna height of 1.0 m and a frequency band of 5.5 GHz.

Figure (12) shows the propagation gain of the directive channel. Two zones can be distinguished. The first one is with a propagation exponent n_1 of 1.943 and the second one with a propagation exponent n_2 of 2.868. In the first zone, the induced fading can be approximated by a Gaussian distribution with $\mu = 0$ and $\sigma = 1.5$ dB. The induced fading of the second zone is approximated by a sum of Gaussian distribution with ($\mu = 0$ dB, $\sigma = 4$ dB) and a Rayleigh Distribution as shown in Figure (13).

Also, the induced fading of the second zone is approximated by a Hypo-Rayleigh distribution (with a = 0.0025 and $\sigma = 0.8$) as shown in Figure (14).
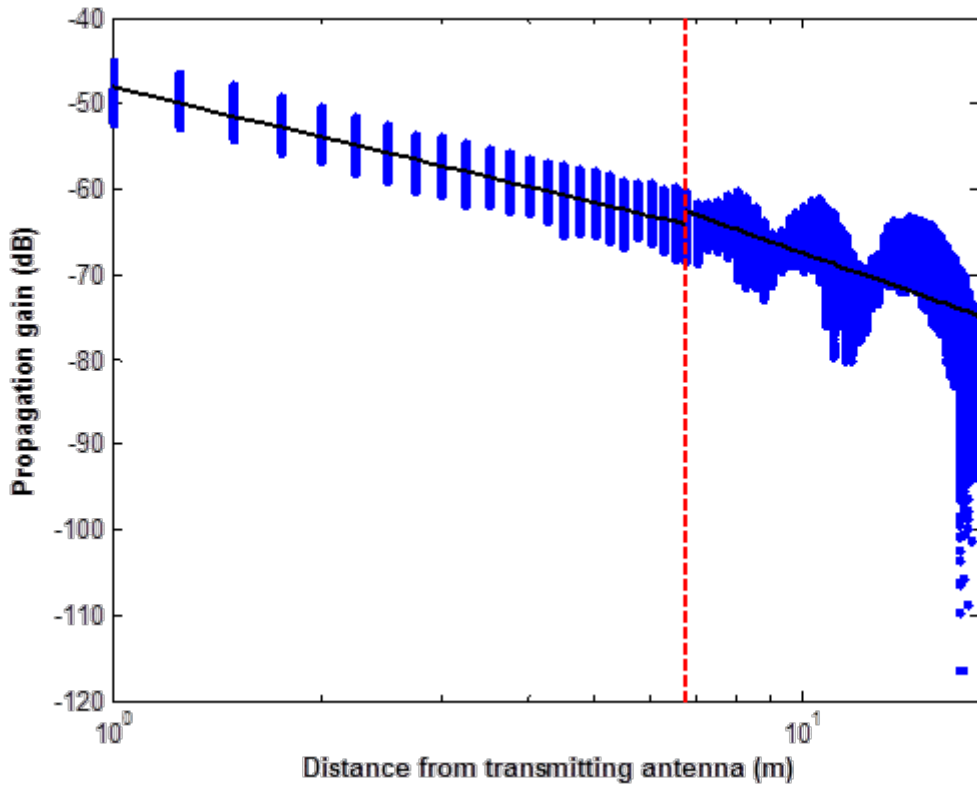

Fig. 12: Propagation gain at antenna height of 1.0 m for the band of 5.5 GHz.
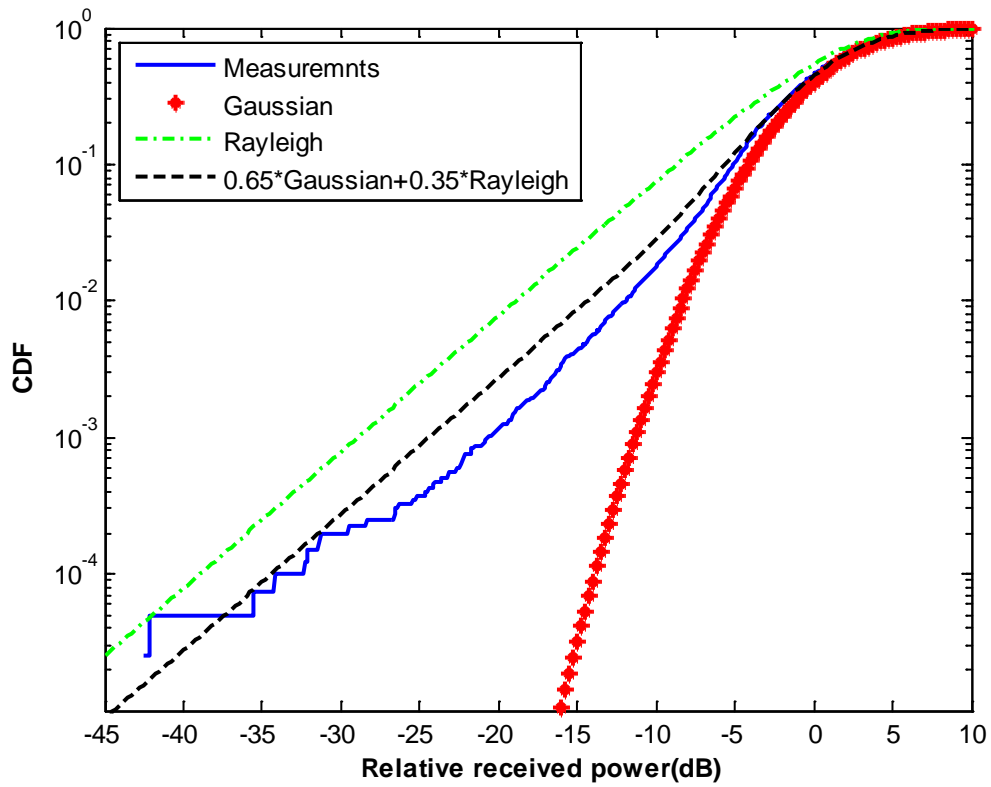
Fig. 13: CDF of the induced fading of the second zone approximated by a combination of Gaussian distribution with Rayleigh distribution for antenna height of 1.0 m at 5.5 GHz band.
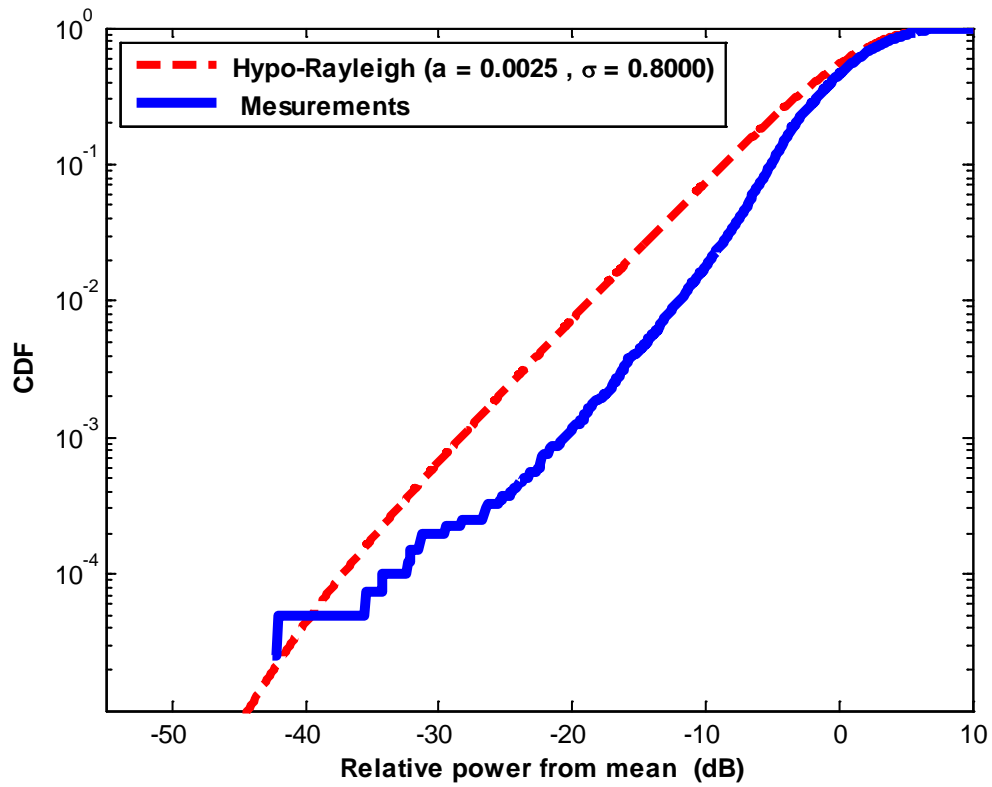
Fig. 14: CDF of the induced fading of the second zone for antenna height of 1.0 m at 5.5 GHz band.

Finally we will present the result for an antenna height of 1.4 m and a frequency band of 5.5 GHz.

Figure (15) shows the propagation gain of the directive channel. Two zones can be distinguished. The first one is with a propagation exponent n_1 of 1.946 and the second one with a propagation exponent n_2 of 2.322. In the first zone, the induced fading can be approximated by a Gaussian distribution with $\mu = 0$ and $\sigma = 1.5$ dB. The induced fading of the second zone is approximated by a sum of Gaussian distribution with ($\mu = -3$ dB, $\sigma = 3.5$ dB) and a Rayleigh Distribution as shown in Figure (16).

Also, the induced fading of the second zone is approximated by a Hypo-Rayleigh distribution (with $a = 0.140$ and $\sigma = 0.500$) as shown in Figure (17).
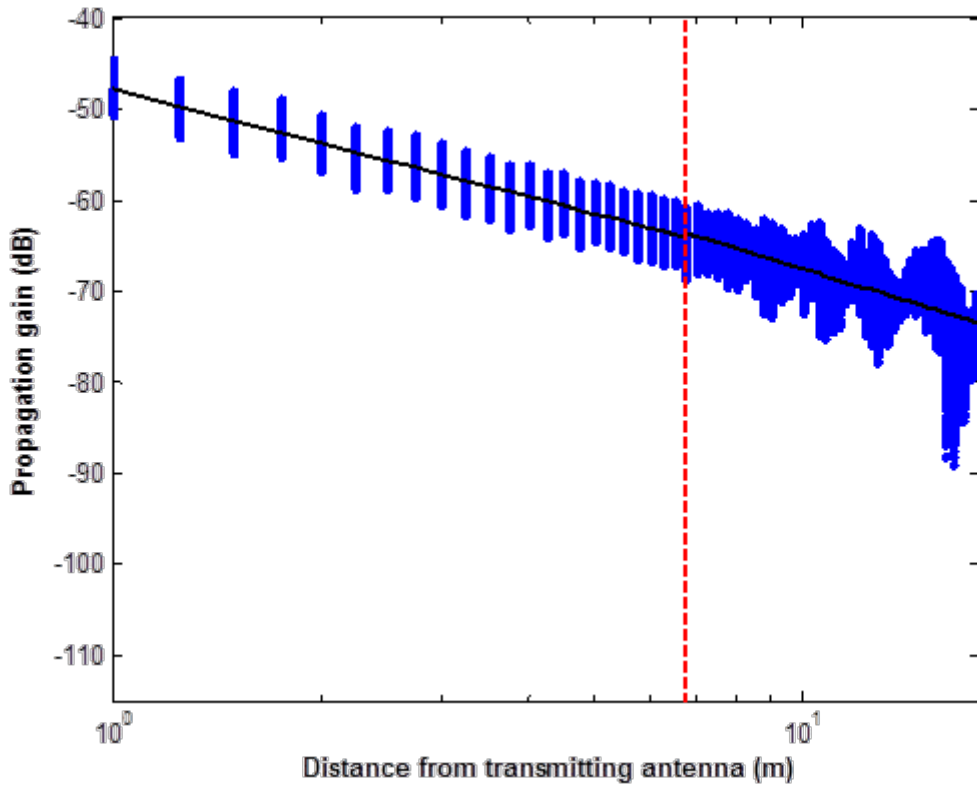

Fig. 15: Propagation gain at antenna height of 1.4 m for the band of 5.5 GHz.
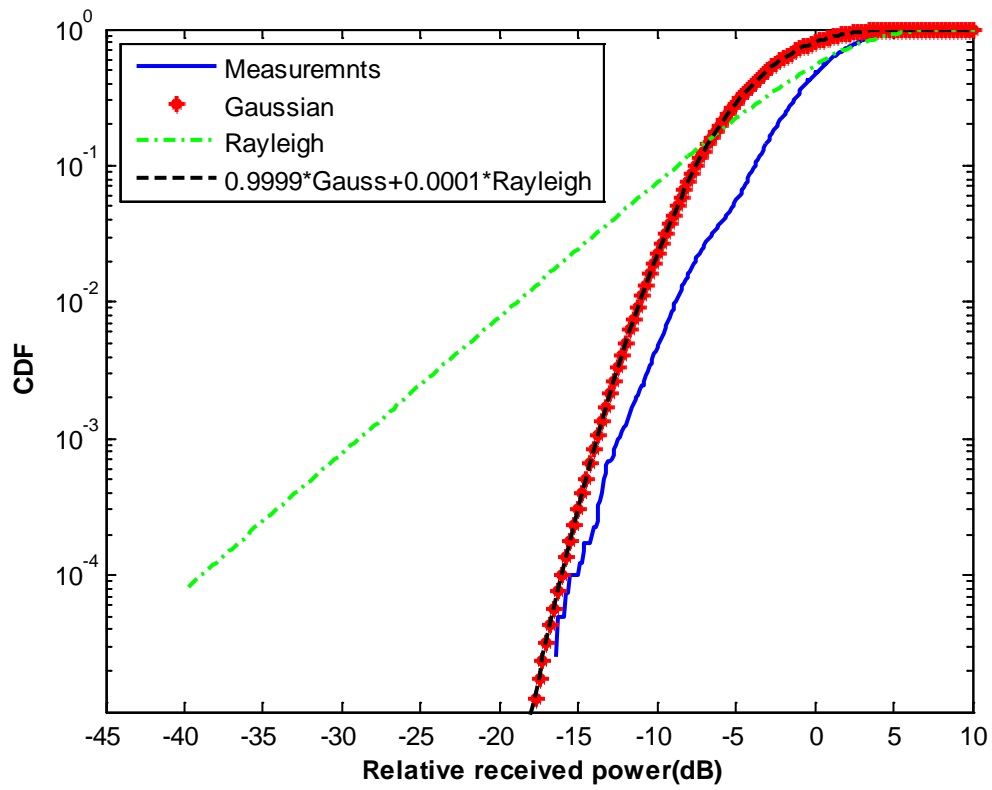
Fig. 16: CDF of the induced fading of the second zone approximated by a combination of Gaussian distribution with Rayleigh distribution for antenna height of 1.4 m at 5.5 GHz band.
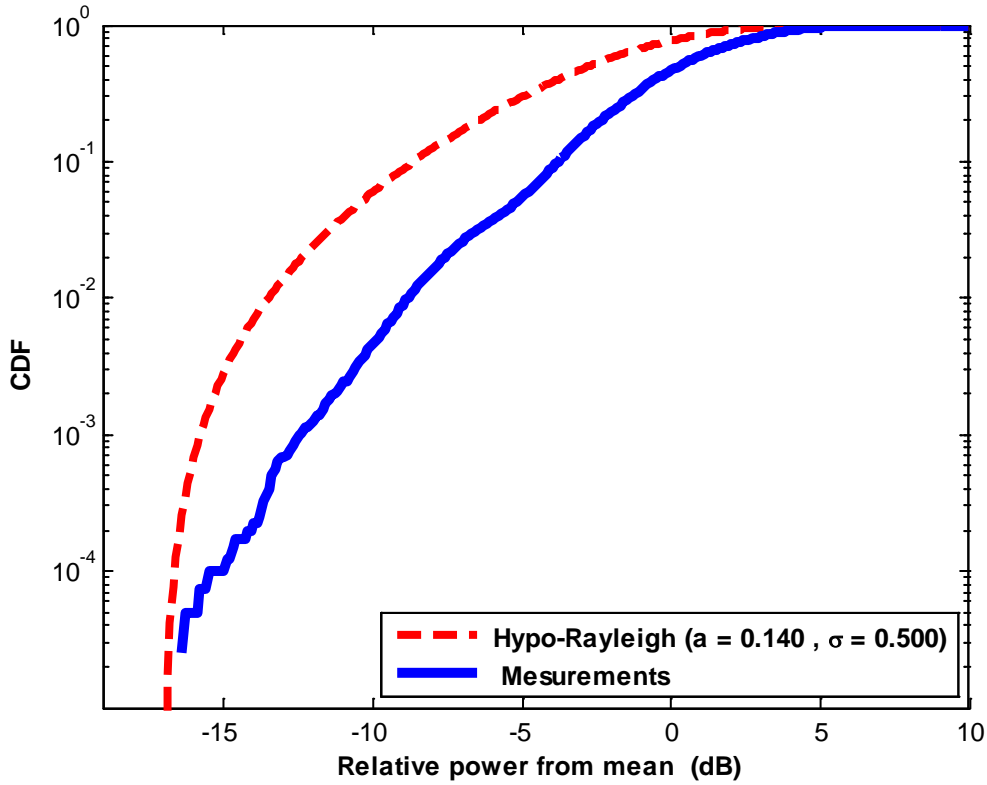
Fig. 17: CDF of the induced fading of the second zone for antenna height of 1.4 m at 5.5 GHz band.

From the above given results, it can be noticed that the severity of the induced fading in the second zone depends on the antenna heights and the operating frequency. Fading will be more severe when the antennas are at lower heights due to the higher reflection from the ground. Higher operating frequency gives arise to more severe induced fading.

5 Conclusions

A new Hypo-Rayleigh distribution has been proposed to model the channel induced fading in the second zone of the propagation zones of indoor directive channel. The directive channel propagation loss in indoor environment at frequency bands of 3.3 GHz and 5.5 GHz has been measured with a channel bandwidth of 200 MHz and 320 MHz respectively has been used. Propagation loss models for indoor environment have been presented. It has been noticed that the propagation loss can

be modelled by a two slopes propagation model. It has been noticed that the first zone of propagation is almost free space propagation zone. The second zone of propagation has a higher deviation from the mean value of propagation loss. The severity of the induced fading of the second zone depends on the antenna height and the operating frequency.

REFERENCES

1. M. Golparvar Roozbahani and E. Jedari, A. A. Shishegar, "A new link-level simulation procedure of wideband MIMO radio channel for performance evaluation of indoor WLANS", Progress In Electromagnetics Research, PIER 83, 13–24, 2008.

2. Tayebi, J. Gomez, F. Saez de Adana, and O. Gutierrez, "The application of ray-tracing to mobile localization using the direction of arrival and received signal strength in multipath indoor environments", Progress In Electromagnetics Research, PIER 91, 1–15, 2009.

3. J. Blas, Prieto , Fernández, R. M. Lorenzo, E. J. Abril , S. Mazuelas, A., S. M. Franco, A.B. Martinez, and D. Bulllid, "A model for transition between outdoor and indoor propagation" Progress In Electromagnetics Research, Vol. 85, 147−167, 2008.

4. Bahillo, and D. Bullido, "A model for transition between outdoor and indoor propagation", Progress In Electromagnetics Research, PIER 85, 147–167, 2008.

5. N. Yarkoni, N. Blaunstein, "Prediction of propagation characteristics in indoor radio communication environment", Progress in Electromagnetics Research, PIER 59, 151-174, 2006.

6. L. Howitt, M.S. Khan, "A mode based approach for characterizing RF propagation in conduits", Progress in Electromagnetics Research B, Vol. 20, 49-64, 2010.

7. Dinesh Tummala, "Indoor propagation modeling at 2.4 GHz for IEEE 802.11 networks", M.Sc Thesis, University of North Texas, December 2005.

8. Emilie Masson et. al., "Radio wave propagation in arched cross section tunnels – Simulations and measurements". Journal of Communications, Vol. 4, No. 4, 276 - 283, May 2009.

9. Erik Kjeldsen and Marshall Hopkins, "An experimental look at RF propagation in narrow tunnels". Scientific Research Corporation (SRC) Atlanta, Georgia.

10. Marina Barbiroli , Claudia Carciofi , Vittorio Degli Esposti , Franco Fuschini , Paolo Grazioso , Doriana Guiducci, Daniel Robalo, Fernando J. Velez, "Characterization of WiMAX propagation in microcellular and

picocellular environments", 2010 Proceedings of the Fourth European Conference on Antennas and Propagation (EuCAP), 1-5, Barcelona, Spain, 2010.

11. Zaballos, G.Corral, A.Carné, and J. L. Pijoan, "Modeling new indoor and outdoor propagation models for WLAN", (On line) Available at: www.salle.url.edu/~zaballos/opnet/OPNET2004b.pdf.

12. J. M. Gorce, K. Runser, G. de la Roche, "FDTD based efficient 2D simulations of Indoor propagation for wireless LAN", (On line) Available at: www. katia.runser.free.fr/Fichiers/GORCE_IMACS_FINAL.pdf

13. C. Nerguizian, C. L. Despins, S. Affes, M. Djadel, " Radio-channel characterization of an underground mine at 2.4 GHz", IEEE Transactions on Wireless Communications, Vol. 4, No. 5, 2441-2453, September 2005.

14. J. Poutanen, K. Haneda, J. Salmi et al., "Analysis of radio wave propagation from an indoor hall to a corridor", IEEE Antennas and Propagation Symposium /USNC/URSI, Vols. 1-6, 2683-2686, 2009.

15. X. H. Mao, Y. H. Lee, B. C. Ng, " Propagation modes and temporal variations along a lift shaft in UHF band", IEEE Transactions on Antennas and propagation, Vol. 58, No. 8, 2700-2709, August 2010.

16. Bazil Taha Ahmed, D. F. Campillo, and J. L. Masa Campos, "Short Range Propagation Model for a Very Wideband Directive Channel at 5.5 GHz Band", Progress in Electromagnetics Research, PIER Journal, Vol. 130, pp. 319-346, 2012.

17. Bazil Taha Ahmed, César Alfredo Naranjo Hidalgo and Josè Luis Masa Campos, "Narrowband Short Range Directive Channel Propagation Loss in Indoor Environment at Three Frequency Bands", Wireless Personal Communications, Vol. 78, pp. 507-520,2014.

Appendix A

The Hypo-Rayleigh induced fading is due to a strong direct ray between the transmitting antenna and the receiving one with lower power indirect rays as shown in Figure A1 which for simplicity shows only two indirect rays. If the indirect rays diminish, the no fading case will be got.
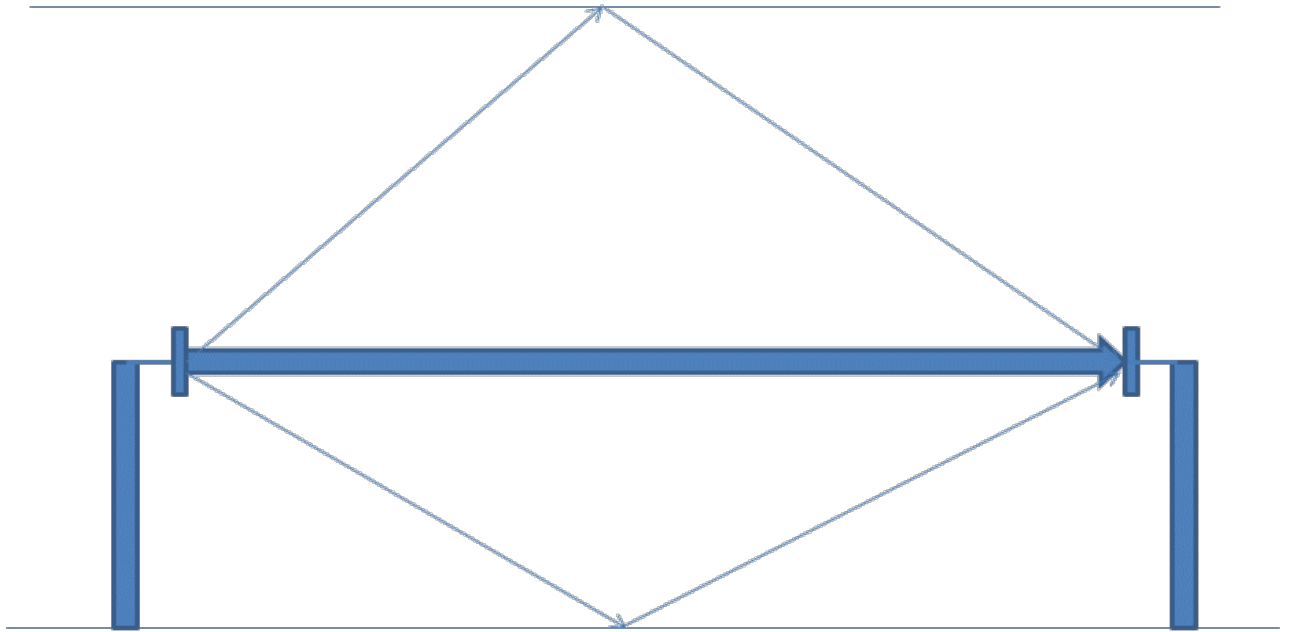

.

Fig. A1: Mechanism of Hypo-Rayleigh induced fading generation in the vertical plane.

The PDF of a Rayleigh distribution is given by:

$$PDF = \frac{r}{\sigma^2} \, e^{-r^2/2\sigma^2} \qquad\qquad r \geq 0 \qquad\qquad (A1)$$

The CDF of the Rayleigh distribution is given by:

$$CDF = 1 - e^{-r^2/2\sigma^2} \qquad\qquad r \geq 0 \qquad\qquad (A2)$$

Subsisting r by (x-a), the PDF of the proposed new distribution (Ahmed Distribution) is given by:

$$PDF = \frac{(x-a)}{\sigma^2} \, e^{-(x-a)^2/2\sigma^2} \qquad\qquad x\text{-}a \geq 0 \qquad\qquad (A3)$$

The CDF of the proposed new distribution (Ahmed Distribution) is given by:

$$CDF = 1 - e^{-(x-a)^2/2\sigma^2} \qquad\qquad x\text{-}a \geq 0 \qquad\qquad (A4)$$

Where a is the deviation parameter.

CDF will be 0 when (x-a) is set to zero mean while it will be one when (x-a) is set to infinity.

This distribution is reduced to the Rayleigh distribution one when a = 0 and it reduces to Hyper-Rayleigh distribution when a is negative. **From A4 it can be noticed that, the CDF value will be 1 when (x-a) goes to infinity.**

Figures A2, A3 and A4 present the PDF of the Hypo-Rayleigh distribution for different values of the parameter (a) for σ of 0.4, 0.8 and 1.2 respectively.

Figures A5, A6 and A7 present the CDF of the Hypo-Rayleigh distribution for different values of the parameter (a) for σ of 0.4, 0.8 and 1.2 respectively. It can be seen that maximum value of CDF is 1.

Figure A8 shows the CDF of the Hypo-Rayleigh, Rayleigh and Hypo-Rayleigh distributions with (a = -0.05, 0 and 0.05 respectively) when σ = 0.8.

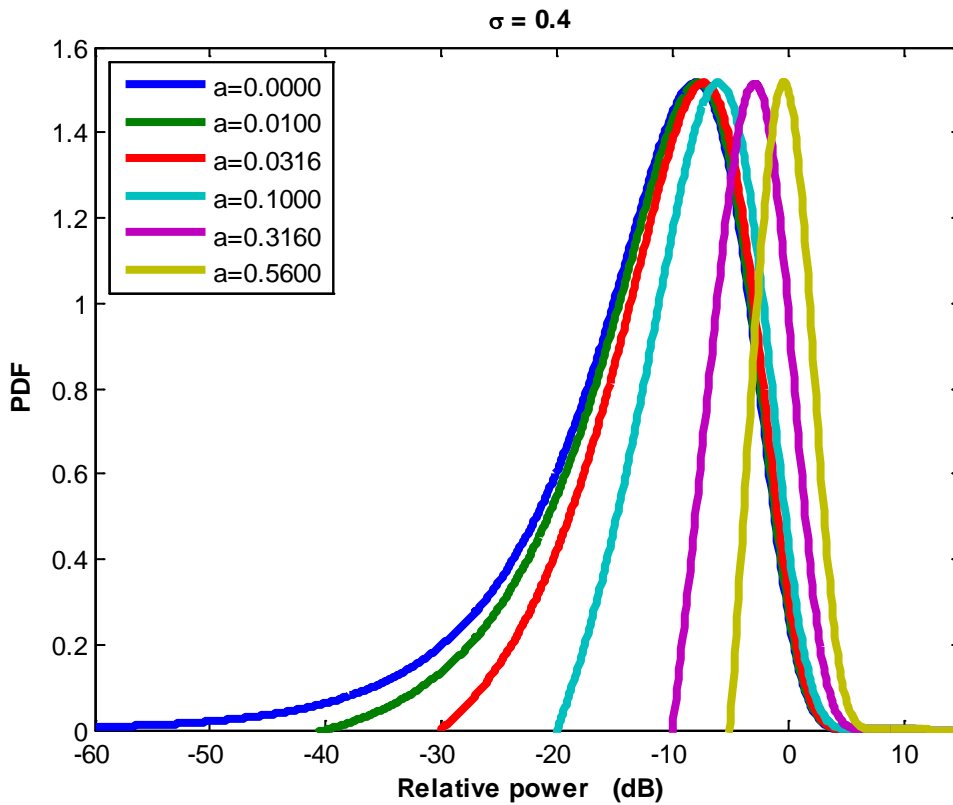The distribution reduced to the no fade case when with a = 1 when σ = 0.0. Figure A9 shows the CDF for this case.

Fig. A2: PDF of the Hypo-Rayleigh distribution for σ = 0.4.
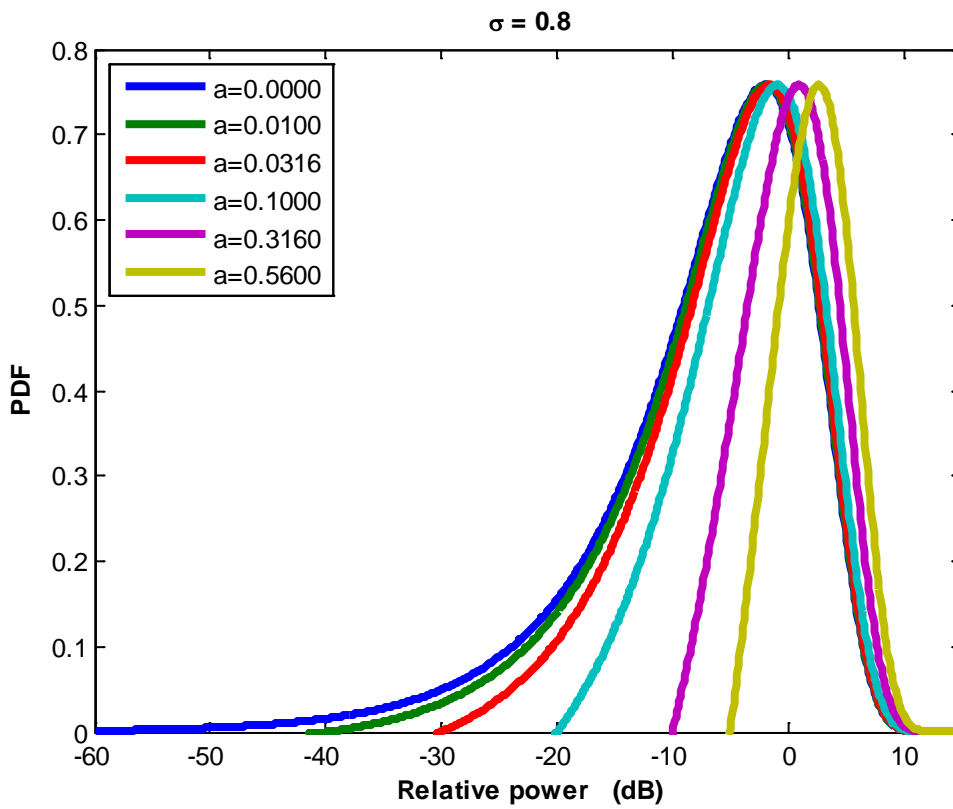
Fig. A3: PDF of the Hypo-Rayleigh distribution for σ = 0.8.
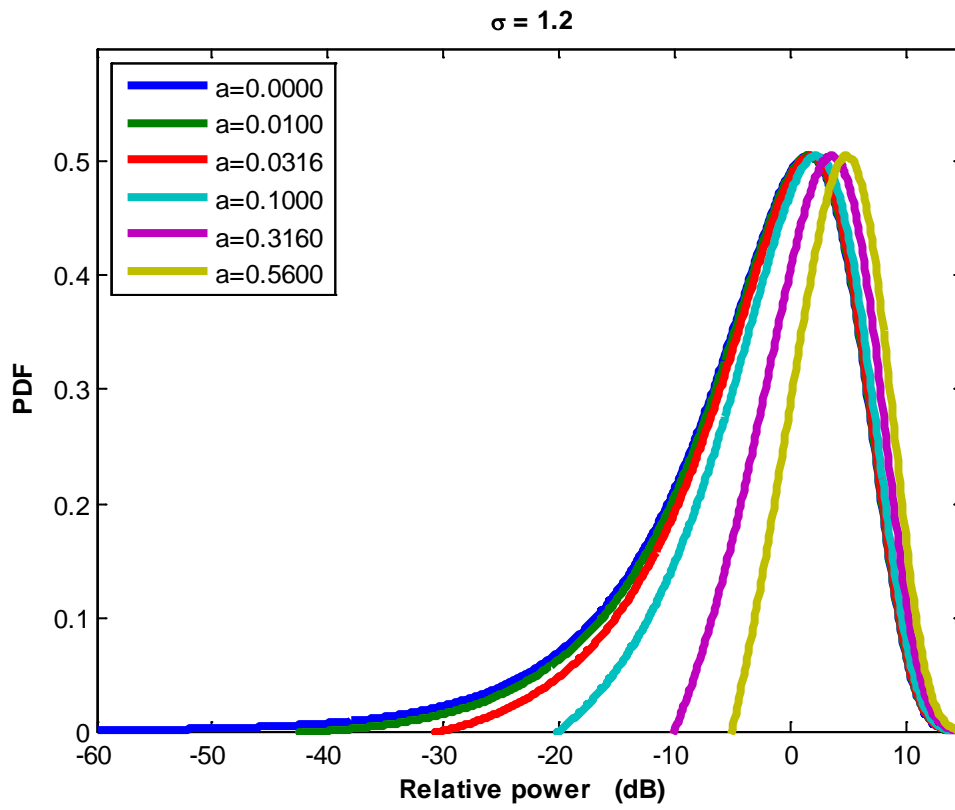
Fig. A4: PDF of the Hypo-Rayleigh distribution for σ = 1.2.
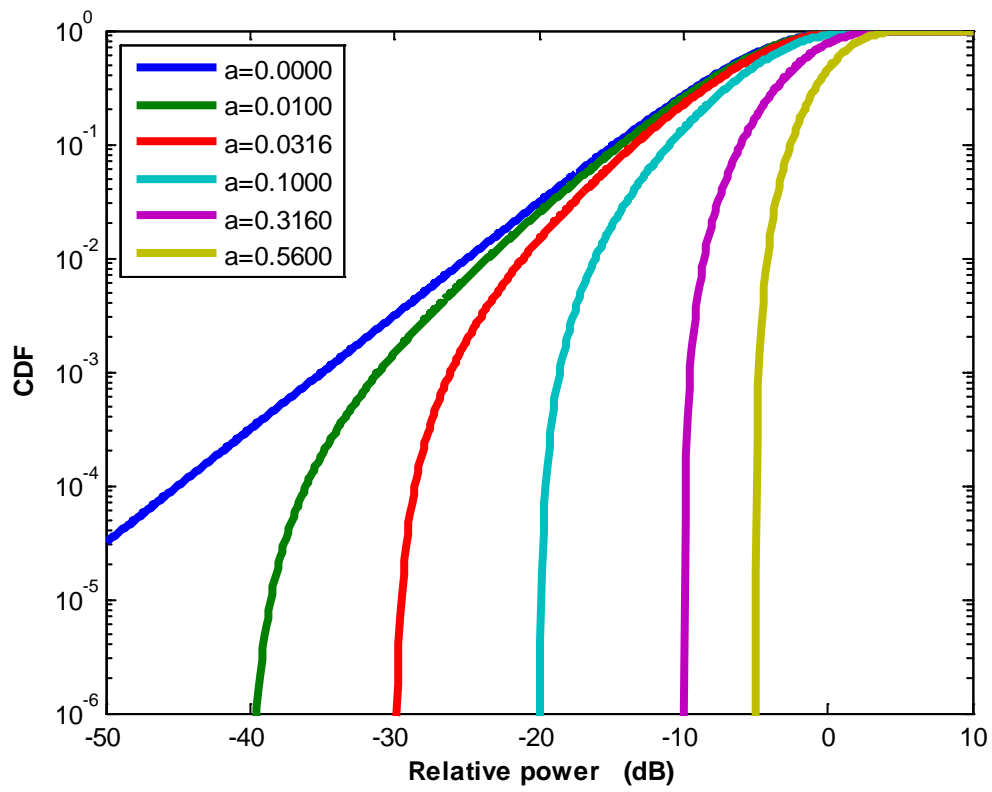
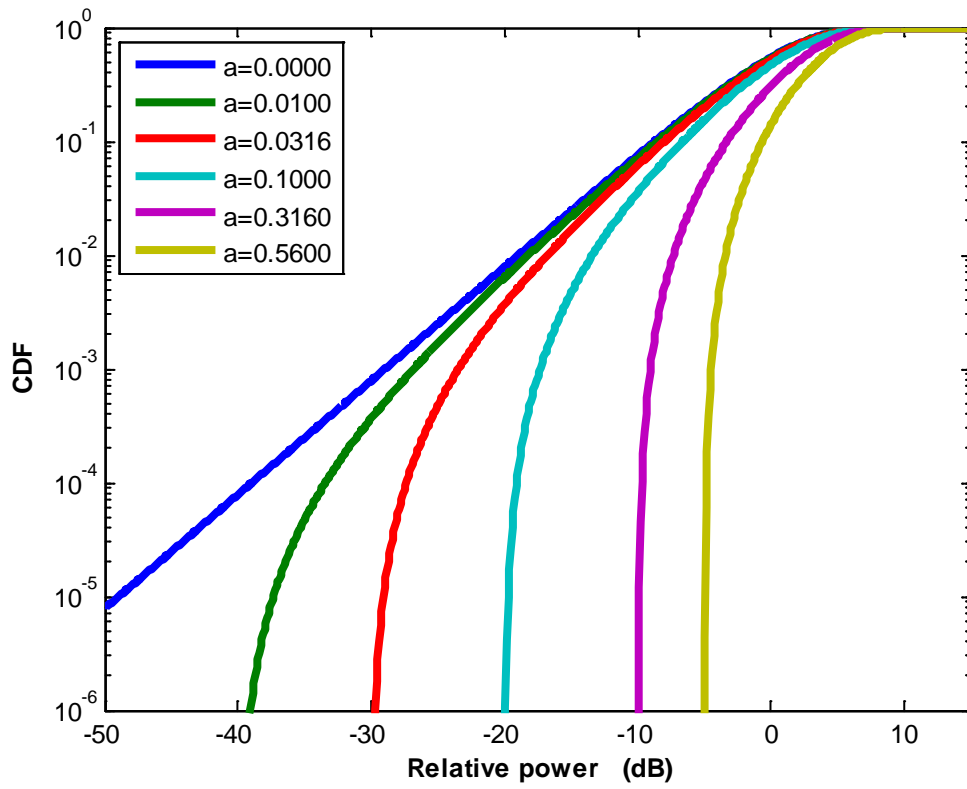**Fig. A5:** CDF of the Hypo-Rayleigh distribution for σ = 0.4.

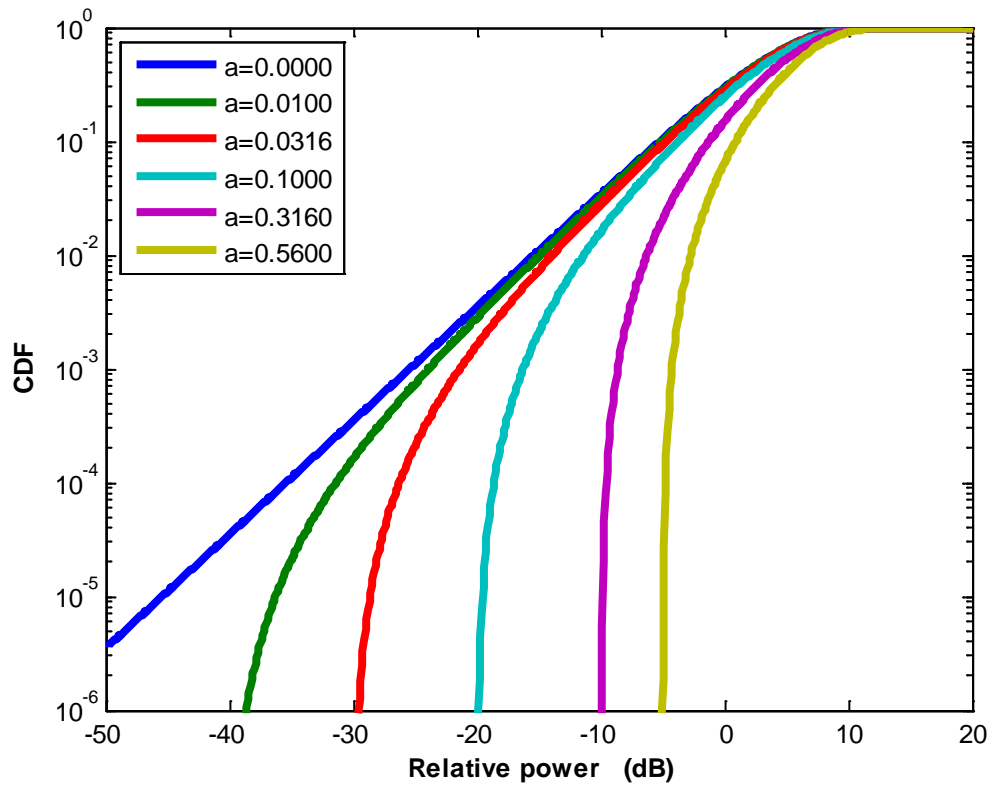**Fig. A6:** CDF of the Hypo-Rayleigh distribution for σ = 0.8.

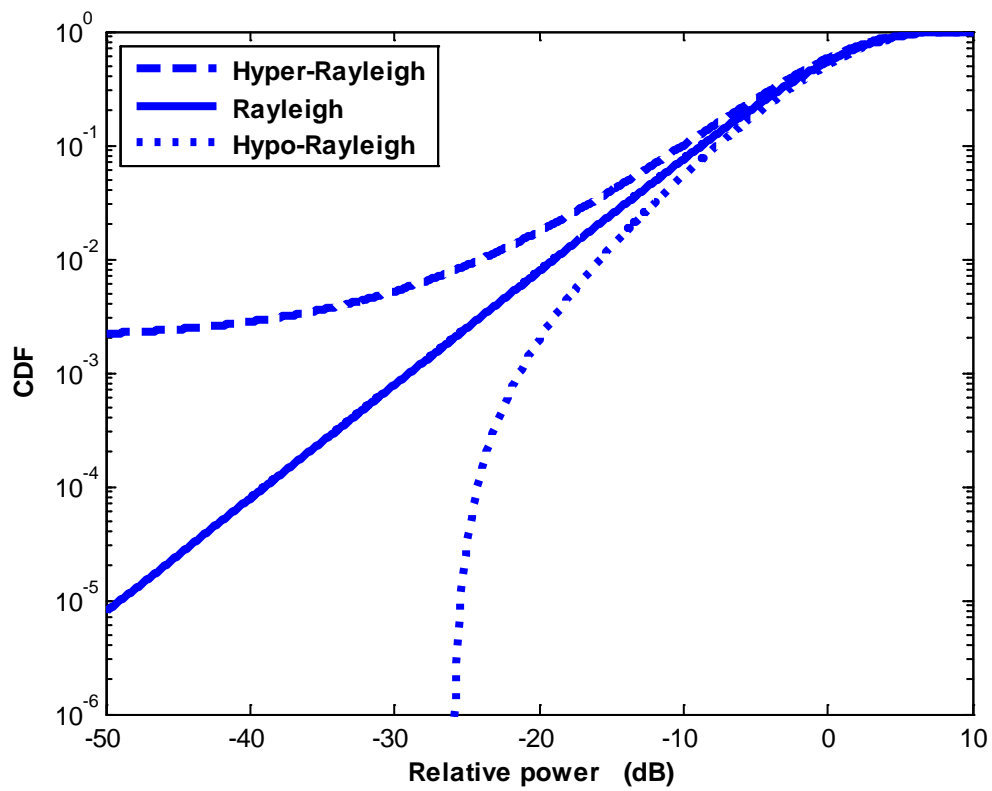**Fig. A7:** CDF of the Hypo-Rayleigh distribution for σ = 1.2.

Fig. A8: CDF of the Hyper-Rayleigh, Rayleigh and Hypo-Rayleigh distributions with (a = - 0.05, 0 and 0.05 respectively) when σ = 0.8.
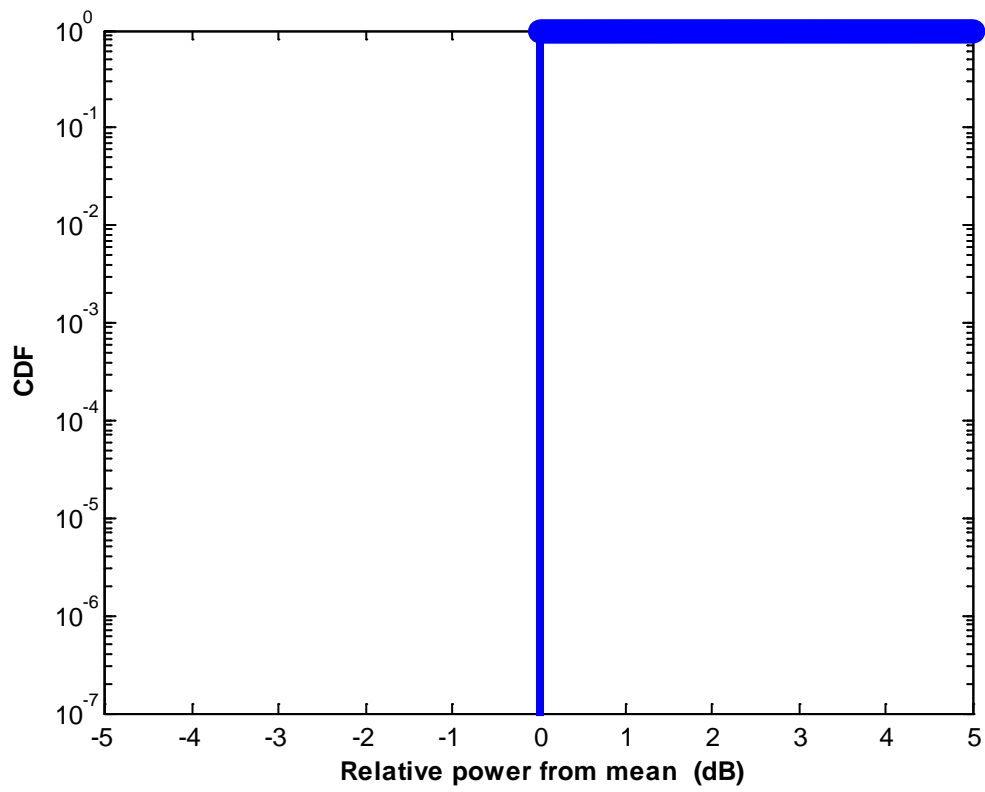
Fig. A9: CDF of the distributions with a = 1 when σ = 0.0 representing the no fade case.